A Modified Impact-increment-based State Enumeration Method and Its Application in Power Distribution Systems

Lukun Ge, Kai Hou, Hongmin Meng, Hongjie Jia, and Ziheng Dong

Abstract—**Reliable planning and operation of power distribution systems are of great significance. In this paper, the impact-increment based state enumeration (IIBSE) method is modified to adapt to the features of distribution systems. With the proposed method, the expectation, probabilistic, and duration reliability indices can be accurately obtained with a lower enumerated order of contingency states. In addition, the time-consuming optimal power flow (OPF) calculation can be replaced by a simple matrix operation for both independent and radial series failure states. Therefore, the accuracy and efficiency of the assessment process are improved comprehensively. The case of RBTS bus 6 system and IEEE 123 node test feeder system are utilized to test the performance of the modified IIBSE. The results show the superiority of the proposed method over Monte Carlo (MC) sampling and state enumeration (SE) methods in distribution systems.**

Index Terms—**Power distribution system, reliability assessment, impact-increment, state enumeration.**

I. Introduction

According to power company statistics, most power outages are caused by component failure in the power distribution system. Therefore, the analysis and evaluation of the distribution system are of great significance [1]. However, the structure of the distribution system is usually complex and diverse, making it difficult to perform such analyses and evaluations. For instance, multiple sections and rings are structured in planning, and the connection of components with other parts through an interconnected switch is quite common. In addition, there are many different kinds of components in the distribution system requiring dedicated attention. This further exacerbates the difficulty in reliability evaluation of the distribution system.

The commonly used reliability evaluation methods that consider the possibility of component failure in the distribution system can be divided into two categories: analytical methods [2] and simulation methods [3].

A typical simulation method is Monte Carlo (MC) simulation [4]-[6]. This method can be used to quantify the impact of related events on the system, especially for complex and large-scale systems. This is because the correlation between computing efficiency and system scale is typically weak, making it more suitable for evaluating the reliability of complex and large-scale systems.

Analytical methods are also commonly used in reliability assessment and can be divided into 3 subcategories: state-space methods [7], system methods [8]-[10], and system state enumeration (SE) methods [11]. The state-space method is used to establish a state-space graph, and then the reliability indices can be obtained by solving the Markov equation. The state-space method can accurately calculate the frequency and duration of each state. However, the calculation is often complicated. The system method is based on the topological structure of the distribution system. This method includes the failure mode effect analysis method [8], the system equivalent method, the shortest path method [9], the minimum cut-set method [10], and the failure diffusion method. In the SE method, the possible states can be directly obtained without considering the transitions between them [11]. Usually, the SE method is more time-efficient than the state-space method. In recent years, there have also been some reliability assessment methods using optimization-based methods. Reference [12] proposes an optimization-based method to compute the standard system-dependent reliability indices. Reliability indices are equivalently determined by an efficient method based on linear programming. Reference [13] proposes an optimization model based reliability assessment method that fully considers the detailed placement and actions of circuit breakers and switches in distribution systems.

It is worth noting that analytical methods are based on the component reliability model and enumerated system failures. One drawback to this method is that it concerns the fact that the number of failure states increases exponentially with the number of system components. Therefore, when the system size increases, the number of failure states increases even more. As a result, the amount of calculation required for ana-

Manuscript received: May 23, 2022; revised: September 28, 2022; accepted: January 30, 2023. Date of CrossCheck: January 30, 2023. Date of online publication: March 16, 2023.

This work was supported in part by the National Natural Science Foundation of China (No. 52077150) and the National Key Research and Development Program of China (No. 2019YFE0118000).

L. Ge (corresponding author), K. Hou, H. Jia, and Z. Dong are with the Key Laboratory of Smart Grid of Ministry of Education, Tianjin University, Tianjin 300072, China (e-mail: gelk@tju.edu.cn; khou@tju.edu.cn; hjjia@tju.edu.cn; dongziheng@tju.edu.cn).

H. Meng is with State Grid Information & Telecommunication Group Co., Ltd., Beijing 102211, China (e-mail: lymhm310@gmail.com).

DOI: 10.35833/MPCE.2022.000297

lytical methods might be too large to be practical for large-scale systems.

Another drawback to the analytical methods is that contingencies with multiple component failures are generally ignored, which leads to the overestimation of the distribution system reliability and is especially implausible in large-scale distribution systems. In large-scale distribution systems, there is a high-possibility for multiple failures due to severe weather condition or misoperation [14]-[16]. In addition, for a complex distribution system such as a multisection, single component failure will not cause a serious blackout accident because the power shortage can be supplied by other sections. However, multiple component failures may cut off both the conventional power supply and transfer path, resulting in much more serious blackout accidents. Therefore, the possibility of multiple component failures should not be ignored [14]-[16]. However, multiple failures tend to dramatically expand the enumerated contingency set, resulting in low efficiency and unacceptable time consumption. Thus, [17] uses the Markov cut-set method to assess the reliability of the distribution system. Some high-probability contingency states are considered in this method, so its reliability outcome is more accurate than that of traditional methods. Reference [18] also uses the Markov cut-set method combining DC optimal power flow (DC-OPF) to assess the reliability of the power system. The DC-OPF is firstly used to determine the cut-set to set order and then the Markov process is used to calculate the reliability indices. Despite the obvious benefits of the two methods mentioned above, they still cannot involve the majority of high-order contingency states. With global climate change, the extreme disasters are increasing, and multiple component failures caused by them are increasingly common. As a result, the obtained reliability indices are mostly lower than their actual values. In recent years, the development of distribution systems has included some new elements such as distributed renewable energy generation, energy storage, and DC distribution systems. In view of the development of these new elements, some researchers have also proposed reliability evaluation methods of distribution system considering those new elements [19]-[22]. However, these assessment methods also do not consider the contingencies with multiple component failures. This shortcoming calls for a new method that can consider as many contingency states as possible to achieve more accurate reliability indices.

A potential solution to the above issue is the impact-increment-based (IIB) method, which is proposed in our previous research [23], [24]. The IIB method is originally developed for transmission systems. It can be used to improve the efficiency of both the IIB state enumeration (IIBSE) and IIB Monte Carlo (IIBMC) methods. Note that the IIBSE and IIBMC are both adapted to large-scale transmission systems [23], [24]. The IIB method can also be integrated with the Lagrange multiplier for further efficiency enhancement [20]. Additionally, the calculation formula of the IIB methods is derived from the traditional SE method by replacing the impact of each enumerated state with its increment. Consequently, the IIB methods can take into account high-order contingency states when enumerating the lower-order states. With these merits, the accuracy and calculation efficiency of the IIB methods are also higher than those of the traditional SE method, especially for expectation indices, e.g., expected energy not supplied (EENS). A high-order contingency reduction method is also proposed herein based on the unique features of the IIB methods mentioned above. This implies that the reliability assessment process is further accelerated. However, the IIB methods do introduce some extra errors in the probabilistic and duration reliability indices, e.g., in the probability of load curtailment (PLC) index used in reliability accessment of transmission system and in the system average interruption duration index (SAIDI) used in reliability accessment of distribution system. This is a drawback that needs to be addressed.

It should be noted that although the IIB method is first developed for transmission systems, it is also suitable for distribution systems, especially for those with radial operation structures. In this paper, the IIBSE method is modified to suit the distribution system, and the mentioned drawback is well addressed. The following are its three contributions.

1) High-order contingency reduction methods are developed for independent and radial series failure states to avoid the time-consuming OPF calculation, which remarkably accelerates the reliability assessment process.

2) Both expectation and duration reliability indices can be accurately obtained by the high-order contingency reduction methods, so that the defect of the original IIBSE (O-IIBSE) method is well addressed.

3) A new identification method is developed especially for distribution systems to identify the categories of high-order failure states.

The rest of the paper is organized as follows. Section II presents the IIBSE method. Section III presents the new category of high-order contingency reduction and the calculation expressions of expectation and probabilistic indices. Section IV presents the new contingency set construction method, failure identification method, and flowchart of the algorithm. Section V presents the case study and Section VI concludes the paper.

II. IIBSE Method

A. Reliability Indices of Distribution Systems

For the original SE method, the reliability index can be obtained by:

$$R=\sum_{k=1}^{N}\sum_{s\in\Omega_A^k}P_sI_s \tag{1}$$

$$P_s=\prod_{i\notin s}a_i\prod_{j\in s}u_j \tag{2}$$

$$u_i=\frac{\lambda_i}{\lambda_i+\mu_i} \tag{3}$$

$$a_i=1-u_i \tag{4}$$

where R is the reliability index; N is the SE order; A is the set of all components; Ω_A^k is the set of all $N-k$ contingencies; s is the system failure state; P_s is the probability of system state s; I_s is the impact of state s, and for the expectation indices such as EENS, I_s is the load curtailment of state s; a_i is the component availability; u_j is the component unavailability; λ_i is the failure rate of the component; and μ_i is the repair rate of the component which can be obtained by the mean time to repair (MTTR) [25].

For probabilistic and duration indices such as PLC and SAIDI, the calculation process includes two steps. First, PLC_i is the PLC of the load point (LP) and can be calculated by (1). I_s in (1) is the load curtailment flag location $I_{f,s,i}$ of each LP, which indicates whether LP i in state s has load curtailment. $I_{f,s}$ can be obtained by:

$$I_{f,s,i}=\begin{cases}1 & I_{s,i}>0\\ 0 & I_{s,i}=0\end{cases} \tag{5}$$

where $I_{s,i}$ is the load curtailment of LP i in state s.

Then the SAIDI can be obtained as:

$$SAIDI=\frac{8760\times\sum_{i=1}^{n}n_i\cdot PLC_i+\sum_{i=1}^{n}n_i\sum_{k=1}^{N}\sum_{s\in\Omega_A^k}\lambda_s t_{s,i}}{\sum_{i=1}^{n}n_i} \tag{6}$$

where n is the number of LPs in the system; n_i is the number of customers in LP i; λ_s is the frequency of state s; and $t_{s,i}$ is the switch operation time of LP i in state s. The first part is the duration caused by failure and the second part is the duration caused by the switch operation which can be calculated by the original method.

B. Fundamental Principle of IIBSE Method

By replacing the impacts and probabilities of system states with their increments, (1) can be converted into an impact-increment form:

$$R=\sum_{k=1}^{N}\sum_{s\in\Omega_A^k}\Delta P_s\Delta I_s \tag{7}$$

where ΔP_s and ΔI_s are the modified probability and the impact-increment of state s, respectively. The two variables can be obtained as:

$$\Delta P_s=\prod_{i\in s}u_i \tag{8}$$

$$\Delta I_s=I_s-\sum_{k=1}^{n_s-1}\sum_{u\in\Omega_s^k}\Delta I_u \tag{9}$$

where u_i is the unavailability of component i; n_s is the number of failed components in state s; ΔI_u is the impact increment of the system state u, which is the lower contingencies of state s; and Ω_s^k is the k^{th}-order subset of state s, determined by:

$$\Omega_s^k=\left\{u\,\middle|\,u\subset s, Card(u)=k\right\} \tag{10}$$

where $Card(u)$ represents the cardinality of state u, when $k=0$, $\Omega_s^k=\phi$.

The difference between SE and IIBSE in the same high-order contingency state is illustrated in Fig. 1. Figure 1(a) shows the load curtailment of a system during multiple failures. Here, 1 and 2 refer to failed components 1 and 2, respectively. The failure durations of the two components overlap. The idea of the original SE method is to evaluate the impacts of the three states, as shown in Fig. 1(b). The three states consist of the $N-1$ state with only one failed component ($s_{\{1\}}$ or $s_{\{2\}}$) and the $N-2$ state with both failed components ($s_{\{1,2\}}$). The load curtailment of the $N-2$ state is higher than the sum of the $N-1$ state. The weight of each state in the reliability indices is the impact of the state. Figure 1(c) shows the idea of the IIBSE method. The impact of $s_{\{1,2\}}$ can be decomposed into the sum of the two $N-1$ state and the increment between $s_{\{1,2\}}$ and $s_{\{1\}}+s_{\{2\}}$. The weight of the $N-1$ state in reliability indices is also the impact of the state, but the weight of the higher-order state is only the increment between $s_{\{1,2\}}$ and $s_{\{1\}}+s_{\{2\}}$. Therefore, the weight of higher-order states is greatly reduced.

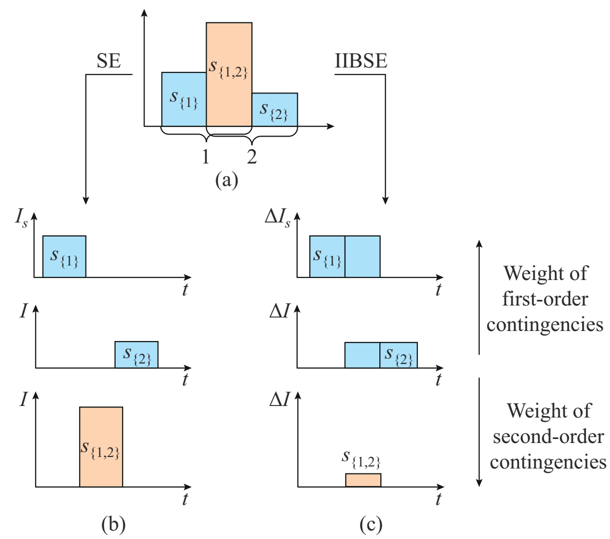

Fig. 1. Difference between SE and IIBSE in the same high-order contingency state. (a) Load curtailment of a system during multiple failues. (b) SE method. (c) IIBSE method.

From the above analysis, it is apparent that the IIBSE method can transfer part of the impact of a high-order contingency state to the corresponding lower-order contingency states. Therefore, it can effectively improve the weight of low-order states in reliability indices. Therefore, it can obtain a more accurate assessment result with a smaller number of enumerated states.

Another benefit of the IIBSE method is that the number of high-order contingency states can be markedly reduced. This independent failure diagram is illustrated in Fig. 2. If a high-order contingency state $s_{\{1,2\}}$ can be divided into two subsets $s_{\{1\}}$ and $s_{\{2\}}$ and the components in $s_{\{1\}}$ and $s_{\{2\}}$ are independent of each other, then the impact increment of $s_{\{1,2\}}$ will always be 0 [22]. Therefore, the expectation indices of these kinds of independent contingency states can be eliminated in the assessment process.

$$\Delta I_{s\{1,2,\dots,n\}}=0 \tag{11}$$

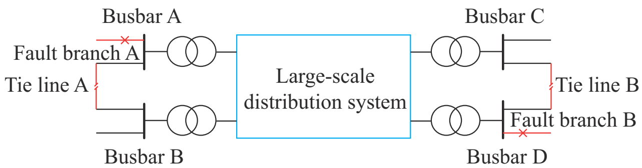

Fig. 2. Independent failure diagram.

III. New Category of High-order Contingency Reduction and Calculation Expressions of Expectation and Probabilistic Indices

The IIBSE method can be utilized to enhance the accuracy and efficiency of the reliability assessment for distribution systems. Unlike a transmission system, if different branches in a large-scale distribution system do not have a tie line connection, the corresponding components are naturally independent of each other. This idea is illustrated in Fig. 2. This feature can make the high-order contingency reduction method more suitable for the distribution system. In addition, the radial characteristics of the distribution system result in a greater reduction of high-order contingency states, so the efficiency can be further improved.

Notably, the original high-order contingency reduction method is based on the additivity assumption of the reliability indices. Therefore, it is more applicable to expectation indices such as EENS. However, the reduction method will inevitably introduce some errors into the probabilistic and duration indices such as SAIDI. This problem can be solved by utilizing the relationship between the high-order contingency state and the low-order contingency state, as shown in Section III-B. In addition, there are many series branches in the distribution system, and the corresponding components are mutually correlated. These states can also be efficiently processed, as shown in Section III-C.

A. Classification of System States

The failure states that can be efficiently processed in a distribution system can be divided into two categories: independent failures and series failures. Each category has two types of indices, i. e., expectation and probabilistic. The original high-order contingency reduction method can still be used to compute the expectation indices of independent states, as shown in Fig. 3. Efficient processing methods are also developed for other categories of radial series failure.

B. Impact-increment of Independent Failure for Probabilistic and Duration Indices

The original high-order contingency reduction method is based on the additivity assumption [22]. This assumption does not hold for probabilistic and duration indices. Therefore, the reduction of mutually independent contingencies will bring extra errors for probabilistic and duration indices, e.g., PLC and SAIDI. For example, in the failure in Fig. 1, if $s_{\{1\}}$, $s_{\{2\}}$, and $s_{\{1,2\}}$ all have load curtailments, the system PLC $I_{f,s\{1,2\}}=I_{f,s\{1\}}=I_{f,s\{2\}}=1$. According to (9), $\Delta I_{f,s\{1,2\},i}\neq 0$ regardless of whether s_1 and s_2 are independent. It is worth noting that accurate probabilistic and duration indices of the whole system can still be obtained by the IIBSE method if the original high-order contingency reduction method is not applied.

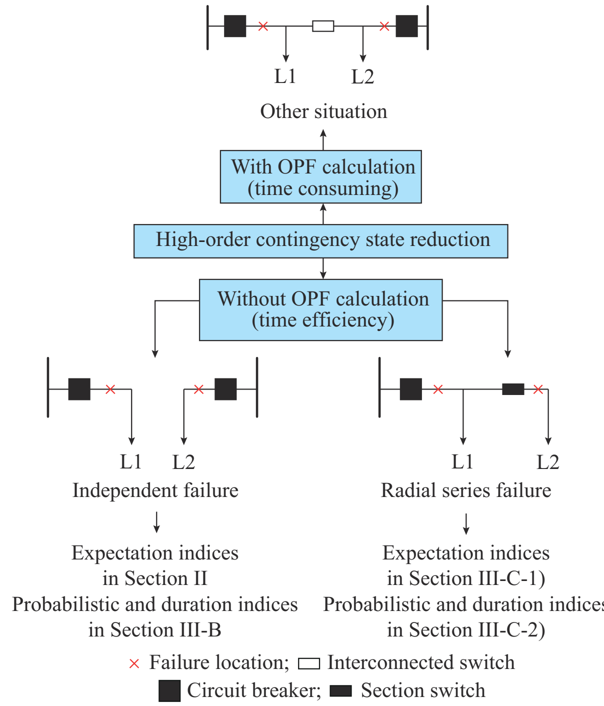

Fig. 3. Categories of high-order contingency reduction method.

However, for the PLC of LPs, the situation is different. It can still be directly calculated by the impacts of each LP in the corresponding low-order contingency states, which means that it can also be obtained without a time-consuming OPF calculation. For an independent high-order contingency state s, LP i will only be within the fault isolation range of the failed component in $s_{\{1\}}$ or $s_{\{2\}}$ for the definition of the independent high-order contingency. Therefore, $I_{f,s\{1,2\},i}=I_{f,s\{1\},i}=1$, $I_{f,s\{2\},i}=0$ or $I_{f,s\{1,2\},i}=I_{f,s\{2\},i}=1$, $I_{f,s\{1\},i}=0$. According to (9), $\Delta I_{f,s\{1,2\},i}=0$. This means that if LPs are within the fault isolation range of the failed component in the independent high-order contingency, $\Delta I_{f,s,i}$ can be obtained by:

$$\Delta I_{f,s,i}=0 \quad \exists I_{u,i}>0, u\subseteq s \tag{12}$$

The switch operation time can also be directly calculated by the impacts of each LP in the corresponding low-order contingency states, and there are possible situations as below.

1) Load point i has switch operation time in the corresponding lower-order states u for which $t_{u,i}>0$. A switch operation time will also occur in the higher-order state s. And similar to load i in fault branch A in Fig. 2, it will not be impacted by fault branch B, so $t_{\{A\},i}>0$, $t_{\{B\},i}=0$. For the high-order contingency, the LP i is still only impacted by branch A, so $t_{\{A,B\},i}=t_{\{A\},i}$.

2) The switch operation time of LP i for all corresponding lower-order contingency states u is equal to 0 (similar to LP i in busbar B or busbar C in Fig. 2). The LP in busbars B and C is not impacted by the failed component in busbars A and D, so $t_{\{A\},i}=t_{\{B\},i}=0$. According to (9), the switch operation time of the independent high-order contingency state s should also be 0, which means $t_{\{A,B\},i}=0$.

In this regard, $t_{s,i}$ can be obtained by:

$$t_{s,i}=\begin{cases}\max t_{u,i} & \exists t_{u,i}>0, u\subseteq s\\ 0 & \forall t_{u,i}=0, u\subseteq s\end{cases} \tag{13}$$

C. High-order Contingency Reduction Method for Radial Series Failures

For the radial distribution system, the schematic diagram of radial series failure is shown in Fig. 4.

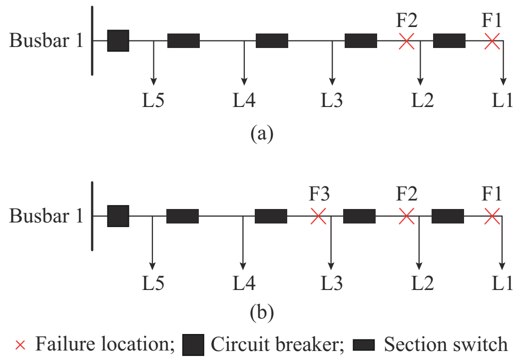

Fig. 4. Schematic diagram of radial series failure. (a) 2-component radial series failure. (b) 3-component radial series failure.

1) Impact-increment of Radial Series Failure for Expectation Indices

For an N-component series failure, the expression of the effect of load curtailment on the impact-increment is:

$$\Delta I_{s\{1,2,\dots,n\}}=(-1)^{n-1}I_{s\{1\}} \tag{14}$$

where $I_{s\{1\}}$ is the impact of the last element in series failures. The mathematical proof is shown in Appendix A.

An example of the 2-component radial series contingency is as follows. The impact of failed components for the expectation indices such as EENS is demonstrated in Fig. 4(a). For component 1, $I_{s\{1\}}=L_1$. Besides, the impact of failed component 2 $I_{s\{2\}}$ equals L_1 plus L_2. Additionally, $I_{s\{1,2\}}=I_{s\{2\}}=L_1+L_2$, so the impact increment of $I_{s\{1,2\}}$ can be given by:

$$\Delta I_{s\{1,2\}}=I_{s\{1,2\}}-\Delta I_{s\{1\}}-\Delta I_{s\{2\}}=L_1+L_2-L_1-L_2-L_1=-L_1=-I_{s\{1\}} \tag{15}$$

Exception index impact-increment of 3 component radial series failures is available in Appendix B.

2) Impact-increment of Radial Series Failure for Probabilistic and Duration Indices

For the probabilistic and duration indices such as SAIDI and PLC, the impact-increment of the load curtailment flag in an N-component series failure can be obtained by:

$$\Delta I_{f,s\{1,2,\dots,n\},i}=(-1)^{n-1}I_{f,s\{1\},i} \tag{16}$$

The mathematical proof is available in Appendix A.

An example of a 2-component radial series contingency is as follows. It can be observed from the failure diagram that $I_{f,s\{1,2\},i}=I_{f,s\{2\},i}$. Therefore, the impact increment of $s_{\{1,2\}}$ is:

$$\Delta I_{f,s\{1,2\},i}=I_{f,s\{1,2\},i}-I_{f,s\{1\},i}-I_{f,s\{2\},i}=-I_{f,s\{1\},i} \tag{17}$$

The switch operation time can be easily found as:

$$t_{s\{1,2,\dots,n\},i}=t_{s\{n\},i} \tag{18}$$

Probabilistic and duration index impact-increment of 3-component radial series failures is available in Appendix C.

IV. New Contingency Set Construction Method, Failure Identification Method, and Whole Algorithm Flow Diagram

In this section, an IIB reliability assessment method is developed, especially for distribution systems. The IIB reliability assessment method is based on the original impact-increment theory in Section II as well as the new contingency state category in Section III. This is done by first dividing the distribution lines into several segments based on the sectional switch to construct the contingency set for reliability assessment. Afterwards, an identification criterion is developed to determine the independent and series contingencies based on topological analysis. Finally, the flow diagram of the proposed method is presented.

A. Distribution System Model

The models of branches and transformers include the start point, end point, resistance, inductance, and other data required by the OPF. The difference between the two models is that the transformer model needs the transformer tap. The switch on the branch is simulated by changing the on-off state of the line. In addition, the reliability data include availability and unavailability data, which can be obtained by (3) and (4).

B. Contingency Set Construction Based on Distribution Line Segment

Constructing the contingency set is the foundation of the reliability assessment of power systems. For the transmission system, the contingency set is built based on the outages of transmission lines and transformers. One inherent challenge regarding this is that lines (or feeders) in a distribution system may have sectionalizing and interconnected switches. Different failure locations in the same line may cause different impacts on the power supply, hence we apply the segment to construct the contingency set for reliability assessment of the distribution system.

A segment is a set of components with common entry components [26], [27]. The entry components are switches or protective devices. From Fig. 5, it is evident that the failure locations within the same segment are likely to cause the same impact. Therefore, the segment can be regarded as the identification component in the contingency set. It can not only cover all possible contingency states but also avoid repetition. The number of identification components in Fig. 5 is decreased from 10 branches and 2 transformers to 5 segments.

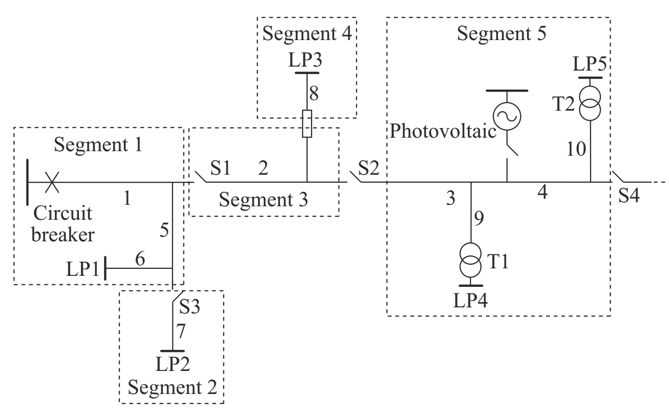

Fig. 5. Structure of segment.

If the segment has x components and y LPs, the failure rate and MTTR of a segment can be obtained by:

$$\lambda_{seg} = \sum_{i=1}^{x} \lambda_i \tag{19}$$

$$\mu_{seg} = \frac{\sum_{i=1}^{x} \lambda_i \mu_i}{\lambda_{seg}} \tag{20}$$

where λ_{seg} is the failure rate of the segment; and μ_{seg} is the MTTR of the segment.

The contingency set is a collection of all possible contingency states, which can be denoted by a set, e.g., {1, 2} refers to the contingency that segment 1 and segment 2 fail.

C. Identification Criteria Based on Topological Analysis

The transmission system is generally ring-structured. Therefore, the independent failures can only be determined by the sensitivity criteria, which inevitably introduces some errors [28]. However, the distribution system is usually ring-structured during the planning and radially structured during the operation, so topological analysis can be used to determine the relationships among faulty components, as shown in Fig. 5. This is possible through the following steps.

Step 1: judge whether the faulty components are in the same station area. If so, go to *Step 2*. Otherwise, they are mutually independent, and their impact increment can be obtained by (11) and (12).

Step 2: record the starting point, search depth, and branch data of all segments in a certain station area by the depth-first search. If the faulty segments are in different branches that started from the same node (segments 2 and 4), the corresponding contingency state {2, 4} is independent, and its impact increment can be obtained by (11) and (12). Otherwise, go to *Step 3*.

Step 3: if the faulty components are in the same branch or front-back branch (segments 3 and 5), the corresponding contingency state {3, 5} is series. Its impact increment can be obtained by (14) and (16). Otherwise, its impact increment can be obtained by OPF calculation and (9).

D. Flow Diagram of Reliability Assessment Method

The flow diagram of the reliability assessment method by IIBSE is shown in Fig. 6.

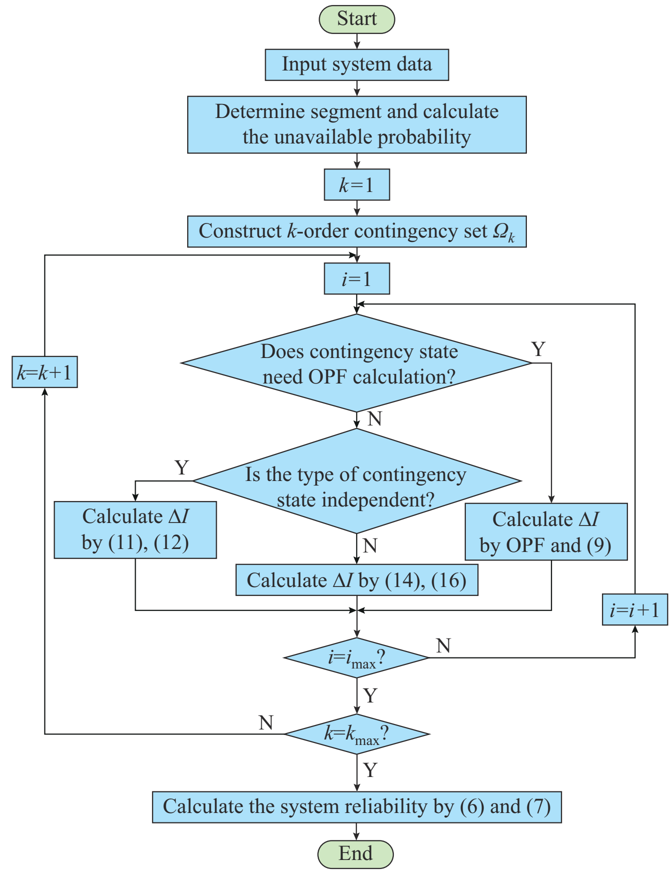

Fig. 6. Flow diagram of reliability assessment method by IIBSE.

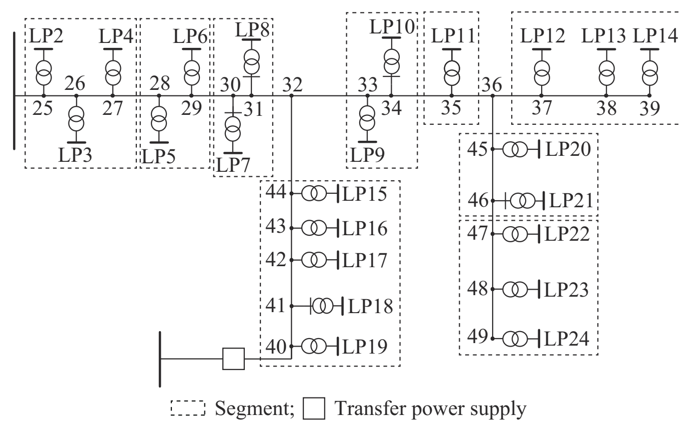

Fig. 7. Segments in modified RBTS bus 6 feeder 4 test system 1.

V. Case Study

A. Modified RBTS Bus 6 Feeder 4 Test System 1

The proposed method is first tested in RBTS bus 6 feeder 4 test system 1 [29], which involves 30 feeder segments, 26 nodes, 23 distribution transformers, 23 LPs, circuit breakers, and disconnections. Node 40 is connected to another feeder by an interconnected switch, whose external characteristics are modelled by a power supply with 4 kW capacity, as shown in Fig. 7. This power supply cannot meet the demand of all loads. The number of consumers at each LP is assumed to be 1. The average failure rate of lines and transformers is set to be 0.13 occurrences per year. MTTR is 8 hours for the line and 15 hours for the transformer.

The MC simulation method with 2×10^6 samples is used as the benchmark. Importantly, the EENS of the benchmark is 102.86 MWh per year, while its SAIDI is 19.66 hours per year. The cut-set method is not used as a benchmark because it calculates the reliability indices only by topology, but in a high-order contingency, power flow can better respond to the real situation. Table I shows the results of the MC, minimal cut-set [30], SE, O-IIBSE, and modified IIBSE (M-IIBSE) methods with various parameters. For the 3 SE-based methods, the obtained indices are more accurate when the enumeration order increases. However, when the enumeration order is higher than 2, a further increase in the enumeration order results in little impact on the assessment outcomes with a concomitant dramatic increase in the computation time. Consequently, the enumeration order should be set to be 2 to balance the accuracy and efficiency.

TABLE I
RESULTS OF MC, MINIMAL CUT-SET, SE, O-IIBSE, AND M-IIBSE METHODS WITH VARIOUS PARAMETERS

Enumeration order	EENS (MWh/year)	EENS error (%)	SAIDI (hour/year)	SAIDI error (%)	Time (s)
MC (2×10^6)	102.86		19.66		1949.1
MC (5×10^4)	105.38	2.44	20.15	2.50	62.7
MC (2×10^5)	103.65	0.76	19.79	0.71	279.6
Minimal cut-set	98.22	4.51	18.86	4.05	0.9
SE ($N-1$)	100.82	1.98	19.31	1.75	3.6
SE ($N-2$)	102.45	0.39	19.82	0.82	94.9
SE ($N-3$)	102.46	0.38	19.83	0.84	1529.5
O-IIBSE ($N-1$)	102.41	0.44	19.47	0.95	4.5
O-IIBSE ($N-2$)	102.46	0.38	19.80	0.69	82.0
O-IIBSE ($N-3$)	102.47	0.37	19.80	0.69	1232.2
M-IIBSE ($N-1$)	102.41	0.44	19.47	0.95	3.6
M-IIBSE ($N-2$)	102.47	0.37	19.77	0.57	72.8
M-IIBSE ($N-3$)	102.48	0.36	19.77	0.57	903.6

It is also shown that the proposed M-IIBSE method is more accurate than the SE and O-IIBSE methods when the enumeration order is identical. It is notable that the O-IIBSE ($N-2$) case has a higher error than the SE ($N-2$) case. This is because the impact increments of series failures are negative, which is rare in transmission systems.

Compared with the minimal cut-set, the accuracy of M-IIBSE is significantly higher than that of the minimal cut-set because the power supply at point 40 cannot meet all the LP demands. The minimal cut-set only uses the topological analysis to calculate the load curtailment, which cannot calculate the load curtailment by insufficient power transfer. The IIBSE can calculate this situation by OPF. In addition, the OPF can consider voltage constraints, which can also increase the accuracy of the M-IIBSE. However, the efficiency of topological analysis is higher than that of OPF, and the operation speed of the minimal cut-set is higher.

Compared with the O-IIBSE, the M-IIBSE has higher accuracy of SAIDI indices. In addition, it is also relatively less time-consuming. In that case, it was found that the SE ($N-1$) case has a 1.98% error rate in EENS, but the M-IIBSE ($N-1$) case only has a 0.44% error rate, which is close to error rate of SE ($N-2$). This is because the weight of the high-order contingency is transferred to the low-order contingency in the IIB method. The error rates in SE ($N-2$) and M-IIBSE ($N-2$) are almost similar to each other and to the benchmark. However, the M-IIBSE method can save as much as 23% of the time performing the same task, making it a better technique. This is because the high-order independent contingency and radial series contingency can use a high-order contingency reduction method instead of a time-consuming OPF calculation. And the time consumption of the M-IIBSE ($N-2$) case is slightly more than that of MC (5×10^4). The accuracy is almost the same.

B. Modified RBTS Bus 6 Feeder 4 Test System 2

If the node of the interconnected switch is changed from node 40 to node 39, the results become slightly different. The segments in modified RBTS bus 6 feeder 4 test system 2 is shown in Fig. 8. The MC case with 2×10^6 samples is used as the benchmark. The EENS is 74.41 MWh per year, while the SAIDI is 13.55 hours per year. The EENS index decreases because most of the loads can obtain power access from both node 1 and node 39. Table II shows the result of M-IIBSE and other methods with different parameters in modified RBTS bus 6 feeder 4 test system 2. The results show that the EENS of the $N-2$ cases is slightly higher than that of the $N-1$ cases. The trend of SAIDI is similar to that in Section V-A. The result of the $N-3$ cases is also similar to that in Section V-A.

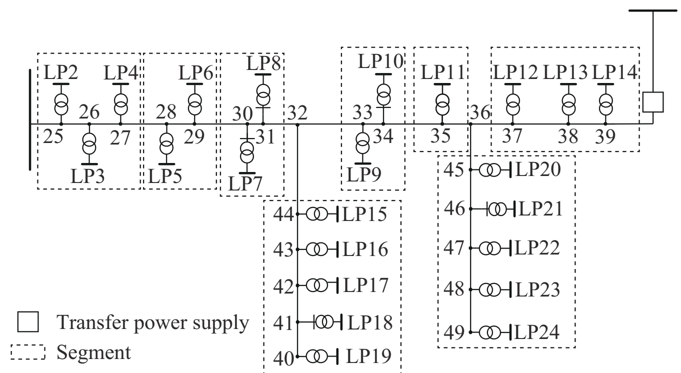

Fig. 8. Segments in modified RBTS bus 6 feeder 4 test system 2.

TABLE II
RESULT OF M-IIBSE AND OTHER METHODS WITH DIFFERENT PARAMETERS IN MODIFIED RBTS BUS 6 FEEDER 4 TEST SYSTEM 2

The maximum enumeration order	EENS (MWh/year)	EENS error (%)	SAIDI (hour/year)	SAIDI error (%)	Time (s)
MC (2×10^6)	71.97		13.55		2169.0
MC (5×10^4)	74.41	3.39	13.98	3.18	81.8
MC (2×10^5)	71.43	0.75	13.45	0.73	257.5
SE ($N-1$)	70.35	2.25	13.26	2.19	3.6
SE ($N-2$)	71.75	0.32	13.62	0.49	99.6
SE ($N-3$)	71.76	0.30	13.62	0.49	1841.1
IIBSE ($N-1$)	71.55	0.58	13.47	0.55	5.3
IIBSE ($N-2$)	71.76	0.30	13.61	0.47	91.3
IIBSE ($N-3$)	71.76	0.30	13.61	0.47	1418.1
M-IIBSE ($N-1$)	71.55	0.58	13.47	0.55	4.3
M-IIBSE ($N-2$)	71.76	0.30	13.59	0.34	84.5
M-IIBSE ($N-3$)	71.77	0.28	13.59	0.34	934.5
Minimal cut-set	69.43	3.52	13.04	3.79	0.9

The results of Table II are largely similar to those of the previous system. For instance, the results of the SE ($N-1$) case have a higher error rate than Section V-A, which is 2.25%. The M-IIBSE ($N-1$) case only has a 0.58% error, which is a number that is higher than that of case 1 but much less than that of the SE ($N-1$) case because the weight of the high-order contingency is transferred to the low-order contingency. The results of the SE ($N-2$) and M-

IIBSE ($N-2$) are almost the same, but the M-IIBSE method can save as much as 15% more time with the high-order contingency reduction method. The time consumption of the M-IIBSE ($N-2$) is almost the same as the time consumption of MC (5×10^4), but the accuracy is almost the same as that of MC (2×10^5). The comparison between O-IIBSE and M-IIBSE is similar to that of Section V-A.

In this case, because the power supply from node 39 cannot supply all LPs, the error of the minimal cut-set is still slightly lower than SE ($N-1$). However, the operation speed is still the fastest among all methods.

The sums of the independent and radial series contingency percentages of RBTS bus 6 feeder 4 test systems 1 and 2 are 27.7% and 21.1%, respectively, as shown in Table III. The values in parentheses represent the percentage of corresponding faults in the total number of $N-2$ faults. This is the reason that the time consumption of the IIB method used in test system 2 is higher than that in test system 1. As mentioned before, the EENS of test system 1 is higher than that of test system 2 because most of the load can obtain power access from both nodes 1 and 39.

TABLE III
COMPARISON OF NUMBER OF DIFFERENT CATEGORIES (N–2 CONTINGENCY) IN TEST SYSTEMS 1 AND 2

Test system	Number of different categories		
	Independent	Radial series	Other situation
1	66 (4.6%)	331 (23.1%)	1034 (72.3%)
2	121 (8.5%)	180 (12.6%)	1130 (78.9%)

C. Modified RBTS Bus 6 System

The third system shown in Fig. 9 is the modified RBTS bus 6 system with 64 lines, 38 distribution transformers, and 40 LPs (LP1-LP40). There are regular open contact switches at the end of feeders F1 and F2. After dividing the feeder area, the number of identification components is reduced to 27, as shown in Fig. 9. The number of consumers at each LP is assumed to be 1. The average failure rates of lines and transformers are set to be 0.14 and 0.02 occurrences per year, respectively.

The result of the MC case with 2×10^6 samples is used as the benchmark. The EENS is 263.46 MWh per year, while the SAIDI is 13.14 hours per year. Table IV shows the result of M-IIBSE and other methods with different parameters in modified RBTS bus 6 system. From the effect of the maximum enumeration order on the reliability index, the errors of EENS and SAIDI in the M-IIBSE ($N-2$) are slightly lower than those of the IIBSE ($N-1$). The time consumption of the M-IIBSE ($N-3$) is significantly higher, which is an observation that can be attributed to the increase in the number of system states. However, the results for EENS and SAIDI are similar to the M-IIBSE ($N-2$) case.

In this case, the power supply in F1 and F2 can fully supply all LPs in F1 and F2. There will be no load curtailment by insufficient power transfer, so the results of the topological analysis and OPF are almost the same. Therefore, the minimal cut-set has almost the same error as the SE ($N-1$), but it is still lower than the M-IIBSE. The operation time of the minimal cut-set is also the fastest of all 5 methods.

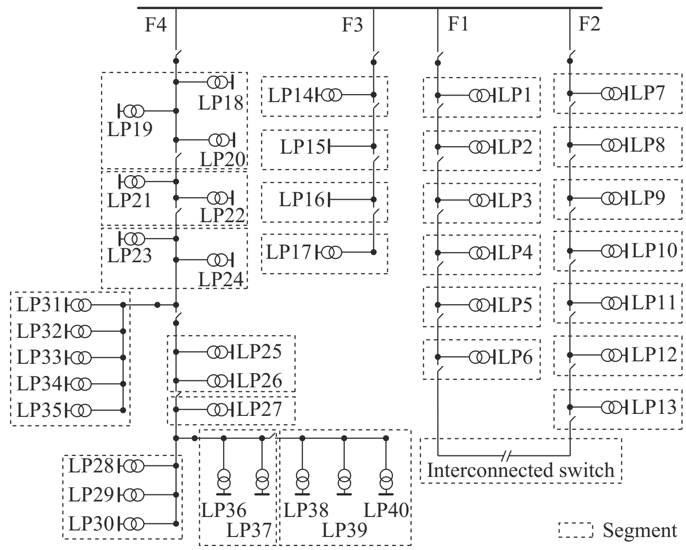

Fig. 9. Segments in modified RBTS bus 6 system.

TABLE IV
RESULT OF M-IIBSE AND OTHER METHODS WITH DIFFERENT PARAMETERS IN MODIFIED RBTS BUS 6 SYSTEM

The maximum enumeration order	EENS (MWh/year)	EENS error (%)	SAIDI (hour/year)	SAIDI error (%)	Time (s)
MC (2×10^6)	263.46		13.14		1992.2
MC (5×10^4)	255.40	3.06	12.76	2.90	55.4
MC (2×10^5)	266.17	1.03	12.98	1.15	203.9
SE ($N-1$)	258.58	1.85	12.91	1.81	17.9
SE ($N-2$)	262.28	0.45	13.21	0.57	808.5
SE ($N-3$)	262.30	0.44	13.21	0.57	37530.2
IIBSE ($N-1$)	262.28	0.45	13.13	0.54	19.6
IIBSE ($N-2$)	262.52	0.36	13.19	0.43	319.7
IIBSE ($N-3$)	262.53	0.35	13.20	0.44	13211.8
M-IIBSE ($N-1$)	262.31	0.43	13.13	0.54	16.2
M-IIBSE ($N-2$)	262.59	0.33	13.17	0.30	188.9
M-IIBSE ($N-3$)	262.61	0.32	13.17	0.30	2097.2
Minimal cut-set	258.57	1.85	12.80	1.80	2.1

The SE ($N-1$) has less error compared with what is observed in Section V-A and V-B, where only a 1.85% error rate in EENS is observed. Compared with other methods, the M-IIBSE ($N-1$) only has a 0.43% error rate, which is less than that of the SE method. The results for the SE ($N-2$) and M-IIBSE ($N-2$) are very similar in terms of error rates. With regard to time consumption, the M-IIBSE method only uses 25% of the time that the SE method uses to perform the same activity. This shows the advantage of efficiency of the M-IIBSE method. The time consumption by the M-IIBSE ($N-2$) case is similar to that of MC (2×10^5). However, the accuracy is much higher in M-IIBSE ($N-2$) compared with the latter method. The comparison between IIBSE and M-IIBSE is similar to the result in Section V-A.

Table V shows the number of different categories ($N-2$ contingency) in modified RBTS bus 6 system. Most of the

$N-2$ contingency states can be calculated quickly because of the structure of the modified RBTS bus 6 system, making the time consumption of M-IIBBSE much less compared with that of the SE method. The number of independent failures increases compared with that in Section V-A and V-B. This observation can be attributed to the increase in the feeder number. The number of radial series failures also increases due to the radial structure of the distribution system. Because of the tie switch between F1 and F2, all $N-2$ contingency states in F1 and F2 need to be calculated by OPF.

TABLE V
NUMBER OF DIFFERENT CATEGORIES ($N-2$ CONTINGENCY) IN MODIFIED RBTS BUS 6 SYSTEM

Case	Number of different categories		
	Independent	Radial series	Other situation
RBTS bus 6	3151 (59.9%)	1120 (21.3%)	982 (18.7%)

D. Modified IEEE 123 Node Test Feeder System

The fourth system shown in Fig. 10 is the modified IEEE 123 node test feeder system with 129 lines and 85 LPs. There are 39 segments in the system. In this paper, the system is simplified and modified. The three-phase system is simplified to a single-phase system and some structures are removed. There are also some switches that are added to the system. The number of consumers at each LP is assumed to be 1. The average failure rates of the lines are set to be 0.14 occurrences per year, and the MTTR is 8 hours. The result of the MC case with 2×10^6 samples is used as the benchmark. Its result for EENS is 1.9168 MWh per year, and for SAIDI, the result is 1.0615 hours per year. Table VI shows the the result of M-IIBSE and other methods with different parameters in modified IEEE 123 node test feeder system. From the effect of the maximum enumeration order on the reliability index, the error rates of EENS and SAIDI in the M-IIBSE ($N-2$) are slightly lower than those of the IIBSE ($N-1$) case. Because of the increase in the number of system states, the time consumption of the M-IIBSE ($N-3$) case is significantly higher than that of M-IIBSE ($N-2$), however, the results of EENS and SAIDI are similar to those of the M-IIBSE ($N-2$) case.

Similar to the case in modified RBTS bus 6 system, the transfer power supply can fully supply all LPs in the whole system. There will be no load curtailment by insufficient power transfer, so the results of the topological analysis and OPF are almost the same. Therefore, the minimal cut-set still has the lowest operation time among all methods. It also has almost the same error as SE ($N-1$), but it is still lower than that of M-IIBSE.

Compared with other methods, the M-IIBSE ($N-1$) only has a 0.41% error rate which is less than that of the SE method. The results for the SE ($N-2$) case and M-IIBSE ($N-2$) case are very similar in terms of error rates. With regard to time consumption, the M-IIBSE method only uses 1/2 of the time that the SE method uses. Nevertheless, with respect to time, the time consumption of the M-IIBSE ($N-2$) case is almost 1/2 that of the MC (1×10^6). However, the accuracy is much higher in M-IIBSE ($N-2$) compared with the latter method.

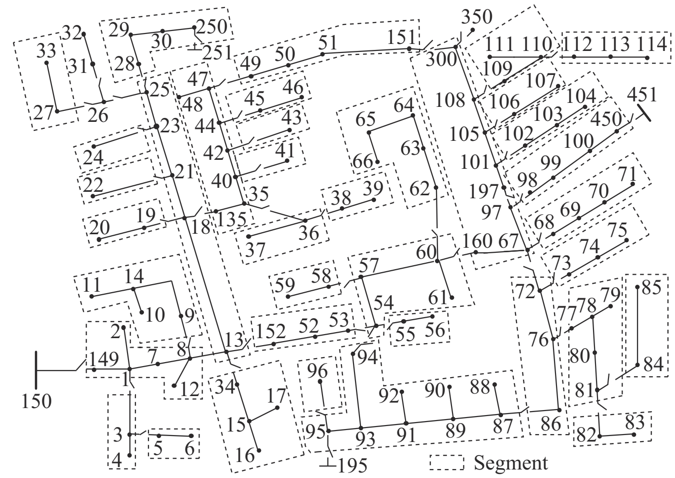

Fig. 10. Segments in modified IEEE 123 node test feeder system.

TABLE VI
RESULT OF M-IIBSE AND OTHER METHODS WITH DIFFERENT PARAMETERS IN MODIFIED IEEE 123 NODE TEST FEEDER SYSTEM

The maximum enumeration order	EENS (MWh/year)	EENS error (%)	SAIDI (hour/year)	SAIDI error (%)	Time (s)
MC (2×10^6)	1.9168		1.0615		2292.2
MC (5×10^4)	1.7939	6.41	0.9969	6.08	66.5
MC (1×10^6)	1.8958	1.09	1.0570	1.05	947.5
SE ($N-1$)	1.8908	1.36	1.0466	1.40	11.9
SE ($N-2$)	1.9102	0.34	1.0570	0.42	813.2
SE ($N-3$)	1.9103	0.34	1.0570	0.42	33955.6
IIBSE ($N-1$)	1.9089	0.41	1.0569	0.43	12.9
IIBSE ($N-2$)	1.9104	0.33	1.0572	0.40	456.7
IIBSE ($N-3$)	1.9104	0.33	1.0573	0.40	18347.5
M-IIBSE ($N-1$)	1.9089	0.41	1.0569	0.43	13.0
M-IIBSE ($N-2$)	1.9104	0.33	1.0577	0.35	450.7
M-IIBSE ($N-3$)	1.9104	0.33	1.0577	0.35	16549.6
Minimal cut-set	1.8908	1.36	1.0467	1.39	3.6

Table VII shows the number of different categories ($N-2$ contingency) in the modified IEEE 123 node test feeder system. Because there are several transfer operations in the system, the number of contingencies calculated by OPF is still the highest in $N-2$. The radial structures in IEEE 123 node test feeder system are short and scattered, so the number of radial series contingencies is much lower than the number of independent contingencies.

TABLE VII
NUMBER OF DIFFERENT CATEGORIES (N–2 CONTINGENCY) IN MODIFIED IEEE 123 NODE TEST FEEDER SYSTEM

Case	Number of different categories		
	Independent	Radial series	Other situation
IEEE 123 node test feeder	2423 (29.81%)	133 (1.64%)	5572 (68.55%)

VI. Conclusion

The O-IIBSE method, which was originally developed for large-scale transmission systems, is modified to accommodate the distribution systems. Compared with the O-IIBSE, the M-IIBSE can process a new kind of high-order contingency, i.e., series failure. Both independent and series failure states can be far reduced without sacrificing the accuracy of the expectation and duration reliability indices. A new identification method is developed to identify the two categories of high-order contingency states that can be reduced.

The modified RBTS bus 6 system and modified IEEE 123 node test feeder system are utilized to test the performance of the M-IIBSE. Compared with traditional MC, SE and IIBSE, the results show that the proposed method is more efficient and accurate. Compared with the minimal cut-set, the M-IIBSE has higher accuracy, especially in distribution systems where shedding loads cannot be fully transferred. It has also been verified in this paper that the larger the system scale is, the more independent and radial series failure states can be identified, and the more contingency states can be reduced. Therefore, the advantage of the proposed method is more obvious in large-scale distribution systems.

There are two main future research directions. The first is the high-order contingency reduction of series failures in meshed structures. The second is the calculation of frequency-related reliability indices in the distribution system because the analytical method performs poorly in sequential analysis.

Appendix A

It is known that this formula holds at $N=2$. It can be proven by mathematical induction that if it holds at $n=k$, it holds for all cases of $n>1$ as long as it can be proven that it holds at $n=k+1$.

$$\begin{aligned}\Delta I_{s\{1,2,\dots,n+1\}}=&I_{s\{1,2,\dots,n+1\}}-(\Delta I_{s\{1,2,\dots,n\}}+\Delta I_{s\{1,2,\dots,n-1,n+1\}}+\dots+\\&\Delta I_{s\{2,3,\dots,n+1\}})-(\Delta I_{s\{1,2,\dots,n-1\}}+\Delta I_{s\{1,2,\dots,n-2,n+1\}}+\dots+\\&\Delta I_{s\{3,4,\dots,n+1\}})-\dots-(\Delta I_{s\{1\}}+\Delta I_{s\{2\}}+\dots+\Delta I_{s\{n+1\}})=\\&I_{s\{1\}}+(-1)^n(C_n^{n-1}I_{s\{1\}}+C_{n-1}^{n-1}I_{s\{2\}})+\\&(-1)^{n-1}(C_n^{n-2}I_{s\{1\}}+C_{n-1}^{n-2}I_{s\{2\}}+C_{n-2}^{n-2}I_{s\{3\}})+\dots+\\&(-1)^1(C_n^0I_{s\{1\}}+C_{n-1}^0I_{s\{2\}}+\dots+C_0^0I_{s\{n+1\}})\end{aligned}\tag{A1}$$

$$C_m^0-C_m^1+C_m^2-\dots\pm C_m^m=0\tag{A2}$$

$$\Delta I_{s\{1,2,\dots,n+1\}}=(-1)^nI_{s\{1\}}\tag{A3}$$

Appendix B

In Fig. 4(b), the impact of faulty component 1 is $I_{s\{1\}}=L_1$, the impact of faulty component 2 is $I_{s\{2\}}=L_1+L_2$, and the impact of faulty component 3 is $I_{s\{3\}}=L_1+L_2+L_3$, $I_{s\{1,2\}}=I_{s\{2\}}=L_1+L_2$, $I_{s\{2,3\}}=I_{s\{3\}}=L_1+L_2+L_3$, and $I_{s\{1,3\}}=I_{s\{3\}}=L_1+L_2+L_3$.

The impact of an increment of $I_{s\{1,2,3\}}$ is:

$$\begin{aligned}\Delta I_{s\{1,2,3\}}=&I_{s\{1,2,3\}}-\Delta I_{s\{1,2\}}-\Delta I_{s\{1,3\}}-\Delta I_{s\{2,3\}}-\Delta I_{s\{1\}}-\Delta I_{s\{2\}}-\Delta I_{s\{3\}}=\\&L_1+L_2+L_3+L_1+L_2+L_1+L_1-L_1-L_2-L_3-L_2-L_1-L_1=L_1\end{aligned}\tag{B1}$$

Appendix C

According to the two-component expression, the impact-increment for a three component system, $\Delta I_{f,s\{1,2\},i}=-I_{f,s\{2\},i}$, $\Delta I_{f,s\{1,3\},i}=-I_{f,s\{3\},i}$, $\Delta I_{f,s\{2,3\},i}=-I_{f,s\{3\},i}$, $I_{f,s\{1,2,3\},i}=I_{f,s\{1\},i}$, can be given by:

$$\begin{aligned}\Delta I_{f,s\{1,2,3\},i}=&I_{f,s\{3\},i}-(-I_{f,s\{2\},i})-(-I_{f,s\{1\},i})-(-I_{f,s\{1\},i})-\\&I_{f,s\{1\},i}-I_{f,s\{2\},i}-I_{f,s\{3\},i}=I_{f,s\{1\},i}\end{aligned}\tag{C1}$$

References

[1] R. Billinton and P. Wang, "Reliability-network-equivalent approach to distribution-system-reliability evaluation," *IEEE Proceedings–Generation, Transmission and Distribution*, vol 145, no.2, pp. 149-153, Mar. 1998.

[2] R. Billinton and W. Li, *Reliability Assessment of Electric Power Systems Using Monte Carlo Methods*. New York: Springer, 1994.

[3] G. T. Heydt and T. J. Graf, "Distribution system reliability evaluation using enhanced samples in a Monte Carlo approach," *IEEE Transactions on Power Systems*, vol. 25, no. 4, pp. 2006-2008, Nov. 2010.

[4] Y. Tao, T. Wei, W. Yue *et al.*, "Reliability assessment of a multi-state distribution system with microgrids based on an accelerated Monte-Carlo method," *IET Generation, Transmission & Distribution*, vol. 12, no. 13, pp. 3221-3229, Jul. 2018.

[5] G. Li, Z. Bie, H. Xie *et al.*, "Customer satisfaction based reliability evaluation of active distribution networks," *Applied Energy*, vol. 162, no.1, pp. 1571-1578, Jan. 2015.

[6] K. Hou, Z. He, Y. Wang *et al.*, "Reliability modeling for integrated community energy system considering dynamic process of thermal loads," *IET Energy Systems Integration*, vol. 1, no. 3, pp. 1-8, Apr. 2019.

[7] K. Hou, H. Jia, X. Xu *et al.*, "A continuous time Markov chain based sequential analytical approach for composite power system reliability assessment," in *Proceedings of IEEE PES General Meeting*, Boston, USA, Jul. 2016, pp. 1-5.

[8] J. Huang, Z. Li, and H. Liu, "New approach for failure mode and effect analysis using linguistic distribution assessments and TODIM method," *Reliability Engineering & System Safety*, vol. 167, no. 1, pp. 302-309, Nov. 2017.

[9] J. Chen, Y. Tao, X. Yue *et al.*, "Fast analytical method for reliability evaluation of electricity-gas integrated energy system considering dispatch strategies," *Applied Energy*, vol. 242, no. 15, pp. 260-272, Mar. 2019.

[10] Y. Liu and C. Singh, "Reliability evaluation of composite power systems using Markov cut-set method," *IEEE Transactions on Power Systems*, vol. 25, no. 2, pp. 777-785, May 2010.

[11] L. Zhao, J. Ma, and Z. Lei, "Power system operation risk assessment based on possibility prioritization search strategy of cascading outage," in *Proceedings of 5th International Conference on Critical Infrastructure (CRIS)*, Beijing, China, Sept. 2010, pp. 1-10.

[12] G. Muñoz-Delgado, J. Contreras, and J. M. Arroyo, "Reliability assessment for distribution optimization models: a non-simulation-based linear programming approach," *IEEE Transactions on Smart Grid*, vol. 9, no. 4, pp. 3048-3059, Jul. 2018.

[13] Z. Li, W. Wu, X. Tai *et al.*, "Optimization model-based reliability assessment for distribution networks considering detailed placement of circuit breakers and switches," *IEEE Transactions on Power Systems*, vol. 35, no. 5, pp. 3991-4004, Sept. 2020.

[14] B. Retterath, S. S. Venkata, and A. A. Chowdhury, "Impact of time-varying failure rates on distribution reliability," *International Journal of Electrical Power & Energy Systems*, vol. 27, no. 9, pp. 682-688, Nov. 2005.

[15] X. Liu, K. Hou, H. Jia *et al.*, "The impact-increment state enumeration method based component level resilience indices of transmission system," *Energy Procedia*, vol. 158, no. 1, pp. 4099-4103, Feb. 2019

[16] S. I. Lim, S. J. Lee, M. S. Choi *et al.*, "Service restoration methodology for multiple fault case in distribution systems," *IEEE Transactions on Power Systems*, vol. 21, no. 4, pp. 1638-1644, Nov. 2006.

[17] M. Al-Muhaini and G. T. Heydt, "A novel method for evaluating future power distribution system reliability," *IEEE Transactions on Power Systems*, vol. 28, no. 3, pp. 3018-3027, Aug. 2013.

[18] Y. Liu and C. Singh, "Reliability evaluation of composite power systems using Markov cut-set method," *IEEE Transactions on Power Systems*, vol. 25, no. 2, pp. 777-785, May 2010.

[19] A. K. Karngala and C. Singh, "Reliability assessment framework for the distribution system including distributed energy resources," *IEEE Transactions on Sustainable Energy*, vol. 12, no. 3, pp. 1539-1548, Jul. 2021.

[20] Z. Liu, K. Hou, H. Jia *et al*., "A Lagrange multiplier based state enumeration reliability assessment for power systems with multiple types of loads and renewable generations," *IEEE Transactions on Power Systems*, vol. 36, no. 4, pp. 3260-3270, Jul. 2021

[21] S. Hao, "Reliability analysis of AC-DC hybrid distribution network based on energy router," in *Proceedings of 2020 5th International Conference on Power and Renewable Energy (ICPRE)*, Shanghai, China, Oct. 2020, pp. 361-365.

[22] K. Hou, H. Jia, X. Yu *et al*., "An impact-increments-based state enumeration reliability assessment approach and its application in transmission systems," in *Proceedings of IEEE PES General Meeting*, Boston, USA, Jul. 2016, pp. 1-5.

[23] Y. Lei, K. Hou, Y. Wang *et al*., "A new reliability assessment approach for integrated energy systems: using hierarchical decoupling optimization framework and impact-increment based state enumeration method," *Applied Energy*, vol. 210, no.1, pp. 1237-1250, Jan. 2018.

[24] M. Naguib, W. A. Omran, and H. E. A. Talaat, "Performance enhancement of distribution systems via distribution network reconfiguration and distributed generator allocation considering uncertain environment," *Journal of Modern Power Systems and Clean Energy*, vol. 10, no. 3, pp. 647-655, May 2022.

[25] W. Li, *Risk Assessment of Power Systems: Models, Methods, and Applications*, 2nd ed. New York: John Wiley & Sons, 2015.

[26] Y. M. Atwa and E. F. El-Saadany, "Guise AC supply adequacy assessment of distribution system including wind-based DG during different modes of operation," *IEEE Transactions on Power Systems*, vol. 25, no. 1, pp. 78-86, Feb. 2010.

[27] N. Flatabo, R. Ognedal, and T. Carlsen, "Voltage stability condition in a power transmission system calculated by sensitivity methods," *IEEE Transactions on Power Systems*, vol. 5, no. 4, pp. 1286-1293, Nov. 1990.

[28] C. Wang, T. Zhang, F. Luo *et al*., "Fault incidence matrix based reliability evaluation method for complex distribution system," *IEEE Transactions on Power Systems*, vol. 33, no. 6, pp. 6736-3745, Nov. 2018.

[29] R. Billinton and S. Jonnavithula, "A test system for teaching overall power system reliability assessment," *IEEE Transactions on Power Systems*, vol. 11, no. 4, pp. 1670-1676, Nov. 1996.

[30] R. Billinton and G. Singh, "Application of adverse and extreme adverse weather: modelling in transmission and distribution system reliability evaluation," *IEEE Proceedings – Generation, Transmission and Distribution*, vol. 153, no. 1, pp. 115-120, Feb. 2006.

Lukun Ge received the B.S. degree in biomedical engineering from Tianjin University, Tianjin, China, in 2015, and the M.S. degree in power energy system from the Cardiff University, Cardiff, UK, in 2016. He is currently pursuing the Ph.D. degree with the Electrical Engineering Department, Tianjin University. His research interests include reliability and resilience assessment of power systems.

Kai Hou received the B.S., M.S., and Ph.D. degrees in electrical engineering from Tianjin University, Tianjin, China, in 2011, 2013, and 2016, respectively. He is currently an Associate Professor with the Electrical Engineering Department, Tianjin University. His research interests include reliability and risk assessments of power systems, integrated energy systems, and smart grids.

Hongmin Meng received the B.S., M.S., and Ph.D. degrees in electrical engineering from North China Electric Power University, Beijing, China, in 2011, 2013, and 2018, respectively. He is currently employed in State Grid Information and Telecommunication Group, Co., Ltd., Beijing, China, as a Senior Engineer. His main research interests include renewable power control, integrated energy system control, and deep learning for power systems.

Hongjie Jia received the B.S., M.S., and Ph.D. degrees in electrical engineering from Tianjin University, Tianjin, China, in 1996, 1999, and 2001, respectively. He is currently a Professor with Tianjin University. His research interests include power reliability assessment, stability analysis and control, distribution system planning and automation, and integrated energy system.

Ziheng Dong received the B.S. degree in electrical engineering from Tianjin University, Tianjin, China, in 2020. She is currently pursuing the M.S. degree with the Electrical Engineering Department, Tianjin University. Her research interests include reliability and risk assessment of power systems and data-driven methods for power systems.